Numerical studies of current generation by radio-frequency traveling waves

Charles F. F. Karney and Nathaniel J. Fisch

Plasma Physics Laboratory, Princeton University, Princeton, New Jersey 08544
(Received 3 January 1979; final manuscript received 7 May 1979)

By injecting radio-frequency traveling waves into a tokamak, continuous toroidal electron currents may be generated. This process is studied by numerically solving the two-dimensional Fokker–Planck equation with an added quasi-linear term. The results are compared with the one-dimensional analytic treatment of Fisch, which predicted a reduced plasma resistivity when high-phase-velocity waves are employed. It is shown that two-dimensional velocity space effects, while retaining the predicted scaling, further reduce the ratio of power dissipated to current generated by about 40%. These effects enhance the attractiveness of steady-state tokamak reactors utilizing this method of current generation.

I. INTRODUCTION

In order to allow tokamaks to run in the steady state, some means of continuously driving the toroidal plasma current must be found. An essential requirement for reactor applications is that the power required to drive the current be only a small fraction of the fusion power output.

Recently,[1] the damping of high-phase-velocity radio-frequency traveling waves has been proposed as a way of driving the toroidal current. The damping of the waves causes the wave momentum to be given to the electrons, resulting in the formation of a velocity-space plateau on the electron distribution function which carries the current. Since the current-carrying electrons are mostly traveling at several times the electron thermal velocity, they collide relatively infrequently and so retain their current for an appreciable time. It follows that the power required to sustain the current is relatively small. The feasibility of the steady-state reactor driven by this means rests crucially on the arguments of Ref. 1 concerning the question of resistivity. In essence, a new resistivity law was advanced in which the power dissipated is proportional to the current rather than the current squared, as in the familiar Ohmic resistivity law. In Ref. 1 it is estimated, on the basis of the new law, that the ratio of radio-frequency (rf) power dissipated to fusion power output is on the order of a few percent for typical reactors.

The analysis of Ref. 1 made use of a one-dimensional Fokker–Planck equation to describe the electrons. Axial symmetry about the magnetic field allows the reduction in the complexity of the problem from three to two velocity dimensions. The reduction from two to one velocity dimension is made under the assumption that the dependence of the electron distribution function on the perpendicular velocity is that of a Maxwellian with the bulk electron temperature. Within the framework of the one-dimensional equations, there is no easy way to check this assumption. In this paper we wish to assess the validity of this assumption by numerically solving for the full two-dimensional effects. In particular, we wish to verify the resistivity law given in Ref. 1. We note that this work is also relevant to the problem of wave heating of a magnetized plasma (e.g., heating a tokamak plasma with lower hybrid waves), although in the instance of heating the objective is to maximize the power dissipation, rather than to minimize the resistivity.

The outline of the paper is as follows: In Sec. II we write the two-dimensional Fokker–Planck equation with an additional quasi-linear diffusion term with which we describe the interaction of the waves with the plasma. We identify w_1 and w_2, the minimum and maximum parallel phase velocities of the rf waves normalized to the electron thermal velocity, as the most important parameters in the problem. In Sec. III we compare the one- and two-dimensional modeling of the problem. The method for numerically solving the two-dimensional Fokker–Planck equation is briefly discussed in Sec. IV. Section V examines, in detail, the solution to the problem for one choice of w_1 and w_2. In Sec. VI we use the results of many runs with different values of w_1 and w_2 to determine the dependence on these parameters of the current, the turn-on time for the current, and the power dissipated. We compare these results with the predictions of the one-dimensional analysis. In particular, we find that while the one-dimensional theory of Ref. 1 correctly predicts the scaling of the ratio of current to power dissipated, this ratio is larger than that given by Ref. 1 by a factor of about 1.7.

II. STATEMENT OF THE PROBLEM

The evolution of the electron distribution function, f, in the presence of rf waves, is given by

$$\frac{\partial f}{\partial t}=\frac{\partial}{\partial v_{\parallel}}D_{\mathrm{rf}}(v_{\parallel})\frac{\partial}{\partial v_{\parallel}}f+\left(\frac{\partial f}{\partial t}\right)_c, \tag{1}$$

where $v_{\parallel}$ is the velocity parallel to the magnetic field, $D_{\mathrm{rf}}(v_{\parallel})$ is the quasi-linear diffusion coefficient, and $(\partial f/\partial t)_c$ is the Fokker–Planck collision term. Following Ref. 1, the quasi-linear diffusion tensor has been reduced to only the $\mathbf{v}_{\parallel}\mathbf{v}_{\parallel}$ term, because current drive mechanisms utilize only the resonance at $\omega/k_{\parallel}$, the parallel wave phase velocity. This is accomplished by choosing the driving frequency, ω, small compared with the electron gyrofrequency, Ω_e. This inequality is always satisfied, for example, by lower hybrid waves. The other

 0031-9171/79/091817-08$00.90

wave-particle resonances[2] then fall in regions of velocity space void of particles. (Note that we have omitted the possible dependency of D_{rf} on $v_\perp$, the velocity perpendicular to the magnetic field. This omission will be discussed later.)

When computing $(\partial f/\partial t)_c$, we will assume that the background distributions of both ions and electrons are nondrifting, nonevolving Maxwellian distributions, in which case $(\partial f/\partial t)_c$ is given, e.g., by Trubnikov.[3] This assumption regarding the collision term has two important implications. Firstly, under this assumption (1) is a linear equation since self-collisions among the non-Maxwellian components of the electron distribution are neglected. This linearization introduces negligible error when the number of non-Maxwellian particles remains small. Secondly, the background electrons represent an efficient energy sink. The evolving test electrons, being in contact with these background electrons of constant temperature, are able to lose the energy imparted to them by the rf waves. Thus, a steady-state distribution of test electrons eventually results. In an experimentally realistic situation, where heat losses eventually balance the heating by rf waves, a similar steady state will result. Of course, in the absence of a heat sink, the electron temperature would increase, leading to more particles resonant with the wave, affecting both the current and power dissipated. Our main interest is to find the resistivity for a given set of plasma parameters. Thus, the assumption of a fixed temperature background electron distribution represents not only a significant mathematical simplification, but a specific framework in which we can pose the questions of current magnitude and resistivity in the steady state.

As written, there are a large number of parameters to be specified in Eq. (1) before it can be solved. These parameters specify both the nature of the wave spectrum and the components of the background distributions. It turns out that the solution space is, for practical situations, insensitive to a number of these parameters, which we now seek to eliminate from consideration.

The three dimensionless parameters governing the collision operator are the mass ratio, m_i/m_e; the temperature ratio, T_i/T_e; and the ion charge state, Z_i. Since $m_i/m_e \gg 1$, whereas $T_i/T_e \sim O(1)$ in all cases of interest, the ions are so much slower than the electrons that their exact velocities are immaterial. For the same reason, the energy transfer to the ion distribution is of order m_e/m_i of the energy lost on the background electron distribution. Thus, for all practical purposes, all problems are nearly characterized by $m_e/m_i = 0$, in which case T_i/T_e is unimportant. Here, we pick $T_i/T_e = 1$ and $m_i/m_e = 1836$, corresponding to hydrogen plasmas, but obtaining results equally applicable to other plasmas such as deuterium or tritium. In contrast to the mass and temperature parameters, the ion charge state is important in Eq. (1). It governs the relative importance of pitch angle to energy scattering, and can have a large effect on the two-dimensional velocity-space structure of the solution to Eq. (1). In this paper, we will pick $Z_i = 1$, which is the case of most relevance to first-generation fusion reactors. In Sec. VI we will, however, briefly discuss the dependence of the solution on Z_i.

Normalizing velocities to $v_{Te} = (T_e/m_e)^{1/2}$ and time to ν_0^{-1}, where

$$\nu_0 = \log\Lambda\omega_{pe}^4/2\pi n_0 v_{Te}^3, \tag{2}$$

Eq. (1) becomes

$$\frac{\partial f}{\partial \tau} = \frac{\partial}{\partial w} D(w) \frac{\partial}{\partial w} f + \left(\frac{\partial f}{\partial \tau}\right)_c, \tag{3}$$

where $\tau = \nu_0 t$, $w = v_\parallel/v_{Te}$, and $D(w) = D_{rf}(v_\parallel)/(v_{Te}^2\nu_0)$. (The notation for the other components of the velocity is $u = v/v_{Te}$, $x = v_\perp/v_{Te}$.)

Having dealt with the parameters describing the collision operator, we now turn to those characterizing the wave spectrum. In general, the wave spectrum may be of arbitrary shape. However, we may partially anticipate the solution of the problem by noting that at very large spectrum amplitudes, the effect of the waves saturates, and the precise wave amplitude is immaterial. Thus, we may neglect the Bessel function dependence[2] of D_{rf} on $v_\perp$ and take D_{rf} to be a function of $v_\parallel$ only, as mentioned earlier. This assumption is strictly valid when $v_\perp \ll \Omega_e/k_\perp$, where $k_\perp$ is the perpendicular wavenumber. However, since the collisional diffusion, against which the quasi-linear diffusion is eventually balanced, decreases at large $v_\perp$, this assumption on D_{rf} is, in fact, reasonable for $v_\perp$ even larger than $\Omega_e/k_\perp$. Thus, we choose

$$D(w) = \begin{cases} D & \text{for } w_1 < w < w_2, \\ 0 & \text{otherwise}, \end{cases} \tag{4}$$

where the constant, D, is chosen large enough for the solution to be insensitive to its precise magnitude. This is, in fact, what occurs in situations of interest such as rf heating or rf-driven tokamak reactors. Thus, in summary, we have pinpointed the important free parameters in the problem as just two, w_1 and w_2, which characterize the spectrum location.

III. COMPARISON WITH THE ONE-DIMENSIONAL MODEL

Equation (3) was considered in Ref. 1 in the high-velocity limit, valid for the resonant and nearby electrons, for which Eq. (3) becomes

$$\frac{\partial f}{\partial \tau} = \frac{\partial}{\partial w} D(w) \frac{\partial}{\partial w} f + \frac{Z_i + 1}{4u^3} \frac{\partial}{\partial \mu}(1 - \mu^2) \frac{\partial f}{\partial \mu} + \frac{1}{2u^2} \frac{\partial}{\partial u}\left(\frac{1}{u}\frac{\partial f}{\partial u} + f\right), \tag{5}$$

where $\mu = w/u$. In Eq. (5) the second term on the right-hand side represents pitch-angle scattering off ions and electrons and the last term represents energy scattering off electrons. It was further assumed in Ref. 1 that the perpendicular velocity-space dynamics play a minor role. Thus, a Maxwellian perpendicular distribution was assumed and Eq. (5) was integrated over that direction obtaining an evolution equation for the parallel velocity distribution, $F(w)$, (Ref. 4)

$$\frac{\partial}{\partial \tau} F(w) = \frac{\partial}{\partial w} D(w) \frac{\partial}{\partial w} F(w) + \frac{2 + Z_i}{2} \frac{\partial}{\partial w} \times \left(\frac{1}{w^3} \frac{\partial}{\partial w} + \frac{1}{w^2} \right) F(w) . \quad (6)$$

Solving for the steady-state distribution, we obtain

$$F(w) = C \exp\left(\int^w \frac{-w\, dw}{1 + 2w^3 D(w)/(2 + Z_i)} \right) , \quad (7)$$

where C is a constant. Now using Eq. (4) in Eq. (7), we see that the one-dimensional solution for the distribution function is flat in the resonant region if, for $Z_i = 1$,

$$w_1^2 D \gg \Delta , \quad (8)$$

where $\Delta = w_2 - w_1$ and we assume that $\Delta > 1/w_1$. This means that the current and power dissipated are independent of D. In most of the cases that we will discuss, we will take $D = \frac{1}{2}$, but we will check that the two-dimensional solution is insensitive to the value of D in Sec. VI.

It should be mentioned that the one-dimensional method of solution represents a model in which the bulk electrons and ions dissipate both the current and the energy of the test distribution. At first glance, this model appears unphysical since ions cannot absorb energy because they are heavy, and since in like particle collisions, the current cannot change. The model, however, is seen to be reasonable upon further inspection. Electron momentum transfer is reasonable because, although the current is not dissipated *per se* in electron-electron collisions, any momentum transferred from the fast electrons to the slow electrons is then quickly dissipated by the ions. Thus, although the momentum transfer between electrons does not immediately affect the current, it allows the ions to collide more often with current-carrying electrons. Ion energy transfer is reasonable because to sustain a given current in any manner against momentum scattering, work must be performed. The non-Maxwellian features in the test distribution resulting from the work on the test electrons are eventually smoothed out by electron-electron collisions. Thus, the electron-ion collisions do not dissipate energy, but, nevertheless, enhance the transfer of energy to the background electrons.

What the one-dimensional model does not account for is that a significant portion of nonresonant electrons can carry current preferentially in one direction. Although the electron-ion collisions produce a nonresonant current-carrying population by scattering electrons out of the resonant region, continued electron-ion scattering tends to produce a canceling current as momentum is further isotropized. The isotropization effect is aborted, however, because electron-electron collisions can slow down electrons before they produce the canceling current. This means that the total current, J, and the ratio of current to power dissipated, J/P_d, should be greater than in the one-dimensional analysis, but the extent of the enhancement must be analyzed numerically, which we now set out to do.

IV. METHOD OF SOLUTION

We rewrite the right-hand side of Eq. (3) as the negative of the divergence of a flux so that Eq. (3) becomes

$$\partial f / \partial \tau = -\nabla_u \cdot \mathbf{S} . \quad (9)$$

Equation (9) is then solved using an alternating-direction-implicit scheme. The integration is carried out in spherical coordinates, u and $\theta = \tan^{-1}(x/w)$. The domain of integration is $u \leq u_{max}$, with a boundary condition that

$$\mathbf{S} \cdot \hat{n} = 0 \quad (10)$$

at $u = u_{max}$. The justification of this boundary condition is, in part, based on the analytical finding that a steady state will, in fact, be reached.[5]

The numerical method is such that the laws of conservation of particles and energy,

$$\frac{\partial}{\partial \tau} \int f d^3u = 0 , \quad (11)$$

$$\frac{\partial}{\partial \tau} \int \frac{1}{2} u^2 f d^3u = \int \mathbf{u} \cdot \mathbf{S}\, d^3u , \quad (12)$$

are exactly obeyed when the integrals are replaced by the appropriate sums.

We choose $u_{max} = 10$ and a grid size of $50 \times 44 (u \times \theta)$. Doubling the number of points in either direction gives about a 1% change in the ratio of current to power dissipated. In most cases we use a time step, $\Delta\tau$, of 0.4.

The steady-state solution of Eq. (9) with $D(w) = 0$ is a Maxwellian

$$f(u) = (2\pi)^{-3/2} \exp(-u^2/2) . \quad (13)$$

However, when we approximate Eq. (9) by a difference equation, then the steady-state solution is given by the recurrence relation

$$f\left(u = u_j + \frac{\Delta u}{2}\right) = f\left(u = u_j - \frac{\Delta u}{2}\right) \frac{1 - u_j \Delta u/2}{1 + u_j \Delta u/2} , \quad (14)$$

where $\Delta u = 0.2$ (the grid spacing in u) and $u_j = j \Delta u$. Equation (14) closely approximates Eq. (13) where $(u_j \Delta u/2)^2 \ll 1$. When numerically solving Eq. (9), we use Eq. (14) as the initial condition at $\tau = 0$ since it is only this "computational Maxwellian" that is nonevolving in the absence of the rf waves.

The quasi-linear diffusion term is turned on with a ramp function over $0 < \tau < 1$. In addition to the w dependence given in Eq. (4), the quasi-linear diffusion coefficient is set to zero for $u > 9.5$ in order to minimize the interaction of the rf with the boundary at $u = 10$.

V. A TYPICAL CASE

In order to appreciate the structure of the solution of Eq. (3), particularly in the steady state, we examine, in detail, a representative case, namely $D = \frac{1}{2}$, $Z_i = 1$, $w_1 = 3$, $w_2 = 5$.

By $\tau = 600$, the solution for this case has reached a steady state. (The change in the current from $\tau = 400$ to $\tau = 600$ is about 1.5%.) In Fig. 1 we show the steady-state solution. In the resonant region, $w_1 < w < w_2$, the

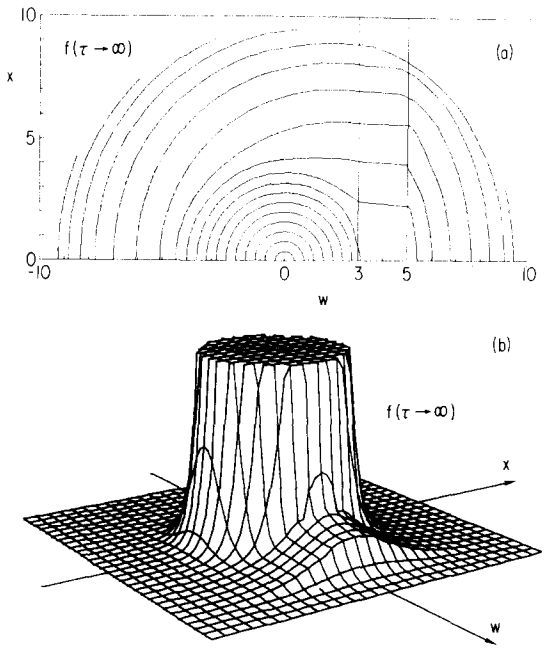

FIG. 1. The steady-state distribution function for $Z_i = 1$, $D = \frac{1}{2}$, $w_1 = 3$, $w_2 = 5$. (a) Contours of constant $f(w, x)$. At the jth contour the magnitude of f is $f_j = (2\pi)^{-3/2} \exp[-(j\Delta v)^2/2]$, where $\Delta v = 0.4$. In this way the contours would be equally spaced circles for a Maxwellian. (b) The surface $f(w, x)$. This is truncated at 0.02 times the maximum of f, in order to show the plateau more clearly. The ranges of w and x plotted are $-7 \leq w \leq 7$ and $-7 \leq x \leq 7$.

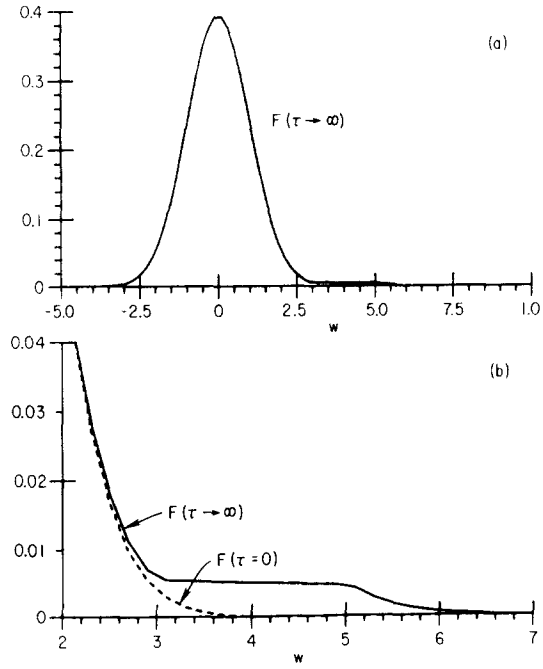

FIG. 2. The parallel distribution function, $F(w)$, for the case shown in Fig. 1. In (b) the vertical scale has been magnified tenfold over that in (a). The dashed line in (b) shows the initial Maxwellian distribution.

electrons are approximately plateaued in the parallel direction. There is significant flattening in the perpendicular direction, also.

By integrating over perpendicular velocity space, we obtain the parallel distribution function, $F(w)$ (Fig. 2), which clearly exhibits the current-carrying plateau. Note that $F(w > w_2)$ drops off more slowly than a Maxwellian distribution with the original temperature would. This is seen more clearly in Fig. 3, where $\log F$ is plotted against parallel energy. We see that $F(w > w_2)$ is roughly Maxwellian with temperature $3T_e$. The influence of pitch-angle scattering produces the same enhanced temperature for $w < -w_2$, although there are far fewer electrons there than in the region $w > w_2$. The rf waves also produce an increase in the perpendicular temperature, as may be seen in Fig. 4. From the figure we see that the perpendicular temperature in the resonant region is about $5T_e$.

In order to see the non-Maxwellian features of the time-asymptotic distribution function more clearly, we subtract from it the Maxwellian distribution characterized by $f(u < w_1)$, i.e., a Maxwellian distribution with the original temperature but a slightly lower density given by $(2\pi)^{3/2} f(u = 0)$. The resulting distribution, $f - f_M$, is shown in Fig. 5.

In order to appreciate the various features of Fig. 5, in Fig. 6 we plot the streamlines of the flux of f. These are defined, in analogy with normal fluid flow, such that at any point the flux, S, in Eq. (9) is tangent to the streamline at that point. The streamlines form closed curves because in the steady state the velocity-space flow is divergence free, i.e., $\nabla_u \cdot S = 0$. The streamline picture is especially useful because it displays the dynamics that are characteristic of the steady state, notwithstanding that the distribution function itself is indeed static.

From the streamlines we can explain the two-pronged dip in the distribution $f - f_M$ near $x = 0$ and $w = w_1$ as seen in Fig. 5. These dips occur where the waves suck electrons out of the Maxwellian region of velocity space, creating local depressions. The electrons drawn into the resonant region are then accelerated in the perpendicular direction by a balance of pitch-angle momentum scattering and quasi-linear rf energy input. Finally, the angle scattering dominates and the electrons are kicked out of the resonant region. The electron-electron collisions cause the streamlines to close upon

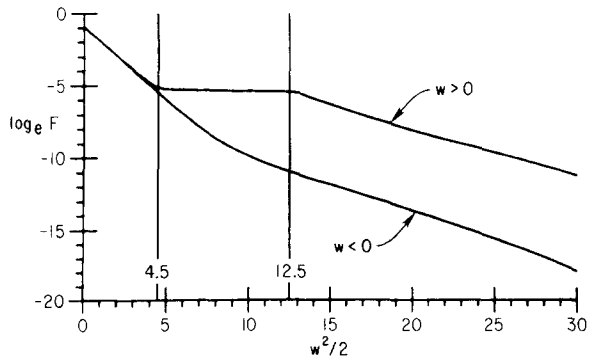

FIG. 3. A Plot of $\log F$ against $w^2/2$ for the case shown in Fig. 1.

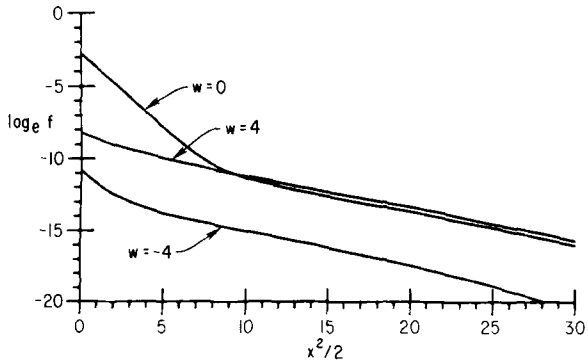

FIG. 4. A plot of $\log f$ against $x^2/2$ for various values of w for the case shown in Fig. 1.

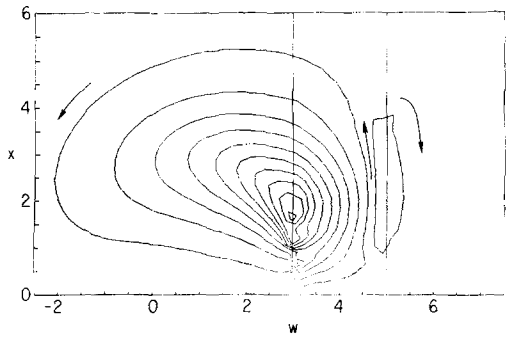

FIG. 6. The streamlines of the flux **S**, for the case shown in Fig. 1. Equal amounts of flux flow between adjacent contours.

themselves before significantly invading the region $w<0$. This is tantamount to the absence of a significant canceling current. The electrons are then collisionally diffused toward the two-pronged depression, where the dynamics are repeated. The depression is off-axis because, at $x=0$, the pitch-angle scattering is only in the perpendicular direction. Incidently, the fact that there is negligible circulation of electrons beyond $u=5$ indicates that the domain in which the problem has been solved is sufficiently large.

We close this section by showing how the current density, J, and the power dissipated evolve in time to the steady state. Figure 7 shows the growth and saturation of J. The turn-on time for the current, as defined by this figure, is about $90\nu_0^{-1}$. In Fig. 8 we show the power dissipated as a function of time. We distinguish two powers

$$P_{rf}=\int \frac{1}{2}u^2\frac{\partial}{\partial w}D(w)\frac{\partial}{\partial w}f\,d^3\mathbf{u}\,, \tag{15}$$

and

$$P_c=\int \frac{1}{2}u^2\left(\frac{\partial f}{\partial \tau}\right)_c d^3\mathbf{u}\,, \tag{16}$$

which, respectively, give the rate of energy gain by the test electrons due to the rf waves and the rate due to collisions with the background distributions (particularly the electrons). The unit of power is $\nu_0 n_0 T_e$. We see that P_{rf} is initially large, but quickly falls to nearly its time-asymptotic value as f plateaus in the resonant region. On the other hand, P_c approaches its asymptotic value much more slowly, on about the same time scale as the current rise. In the steady state, we have

$$P_{rf}(\tau\to\infty)=-P_c(\tau\to\infty)\equiv P_d\,, \tag{17}$$

where the power gained from the rf is exactly balanced by power lost to the background distributions. One interesting feature of P_c is that, just after the rf waves are turned on, it is positive. This is because the background electrons must supply energy to fill in the plateau formed by the waves, while the number of particles in the resonant region is still too small to effectively heat the background electrons.

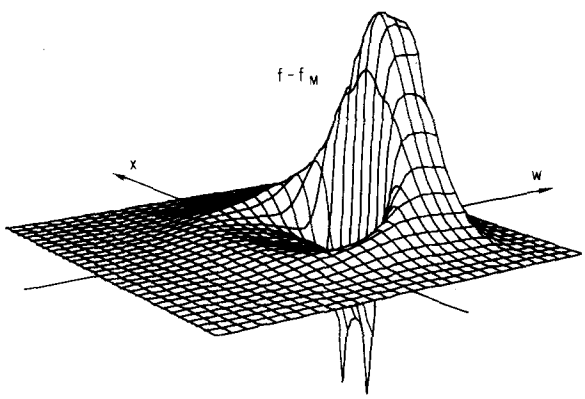

FIG. 5. The non-Maxwellian part of the electron distribution function, $f-f_M$, for the case shown in Fig. 1. The temperature and density of f_M are those characteristic of f for $u<w_1$. The ranges of w and x plotted are $-7\leq w\leq 7$ and $-7\leq x\leq 7$.

VI. CHECKING THE ONE-DIMENSIONAL ANALYTIC THEORY

In this section we wish to check the predictions of the one-dimensional analytic theory regarding the steady-state current, the turn-on time of this current, and the power dissipated in sustaining this current. In the limit $w_1\gg 1$ and $Dw_1^2\gg\Delta\gg 1/w_1$, which assures substantial deviation from a Maxwellian distribution with an essentially flat resonant region, it may be found from Eq. (7) that

$$J=\int_{-\infty}^{\infty} wF(w)\,dw=\frac{\exp(-w_1^2/2)}{(2\pi)^{1/2}}\Delta\left(\frac{w_1+w_2}{2}\right), \tag{18}$$

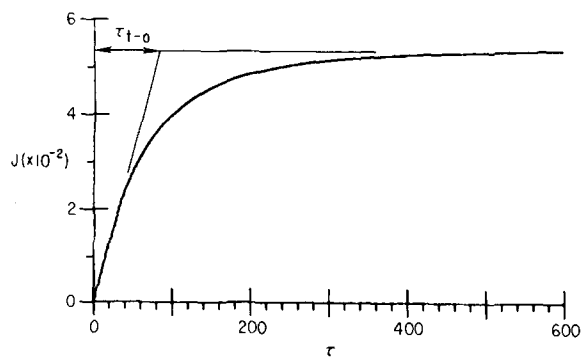

FIG. 7. The temporal evolution of the current, J, for $Z_i=1$, $D=\frac{1}{2}$, $w_1=3$, and $w_2=5$. The unit of current is en_0v_{Te}. The definition of τ_{t-0} is also shown.

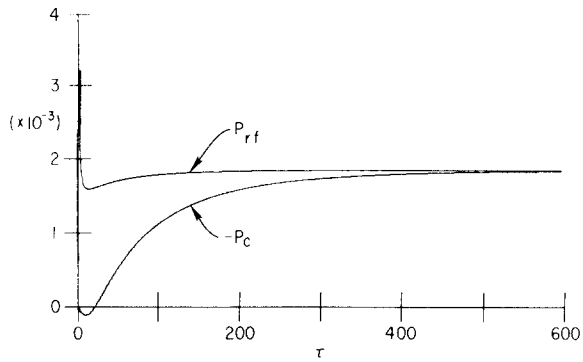

FIG. 8. A plot showing the variation of P_{rf} and P_c [see Eq. (15) and (16)] with time for the case given in Fig. 1. The unit of power is $\nu_0 n_0 T_e$.

$$P_d = -\int_{w_1}^{w_2} wD\frac{dF}{dw}\,dw = \alpha\,\frac{\exp(-w_1^2/2)}{(2\pi)^{1/2}}\log\left(\frac{w_2}{w_1}\right), \tag{19}$$

where $\alpha = (2 + Z_i)/2$. J is expressed in units of $en_0 v_{Te}$, and P_d in units of $\nu_0 n_0 T_e$. The turn-on time for this current given in Ref. 1 is

$$\tau_{t\text{-}o} = \Delta w_1^2/\alpha\,. \tag{20}$$

Our aim is to ascertain the accuracy of Eqs. (18)–(20). We ran approximately 50 cases with $D = \frac{1}{2}$ and $Z_i = 1$ spanning the parameter space $3 \le w_1 \le 6$ and $\Delta = 0.5$, 1, 1.5, 2, and 3. The results are summarized in Figs. 9–11.

Figure 9 shows the numerical results for J, displaying excellent agreement with the prediction, (18), of the one-dimensional theory. Close agreement was to be expected simply because of the predominance of the exponential in Eq. (18). Closer inspection of Fig. 9 reveals that at low w_1 the current is somewhat higher than predicted, whereas at higher w_1 the current is somewhat lower than predicted by one-dimensional theory. The drop in the current at high w_1 is due to the numerical method of solving the problem. There are two numerical limitations that could come into play. One is that the boundary at $u = 10$ in the numerical code, where the boundary condition, (10), is imposed, somewhat restricts the amount of perpendicular velocity space that is available to carry current, which, of course, preferentially affects the high w_1 cases. A second limitation, affecting electrons in a similar manner, is the numerical version of a Maxwellian distribution. The "computer Maxwellian," given by Eq. (14), drops off slightly more rapidly than a true Maxwellian, the discrepancy becoming serious when $u\Delta u \sim 2$. Since we have $\Delta u = 0.2$, the velocity space is effectively restricted even before $u = 10$, so that, in our case, the second limitation is more serious than the first. Plugging in the "computer Maxwellian," rather than the true Maxwellian, into Eq. (18), in fact, fully accounts for the less than predicted current.

It remains that the numerically found current is slightly more than predicted at low w_1 (as, indeed, would also be the case at high w_1 were it not for the numerical procedure). This enhancement of the current is due to the significant portion of the current that is carried by nonresonant electrons, i.e., electrons outside of the region $w_1 < w < w_2$. This enhanced current, occurring especially in the region $u > w_1$, is a fully two-dimensional effect and could not have been predicted by a one-dimensional theory. Nevertheless, it should not be overlooked that the one-dimensional theory, (18), predicts the current generated, quite well.

In Fig. 10 we show the turn-on time for the current. While it does scale as w_1^2, as predicted by the one-dimensional theory, (20), the dependence on Δ is more like $\Delta^{1/2}$ than like Δ. An approximate fit to the numerical results is given by

$$\tau_{t\text{-}o} \approx 6\Delta^{1/2} w_1^2 \tag{21}$$

(see Fig. 10). For Δ characteristic of practical applications, Eq. (21) represents a substantially longer turn-on time than predicted by Eq. (20).

The most important prediction of Ref. 1 concerns the current per unit power dissipation. From Eqs. (18) and (19), we see that

$$J/P_d = \langle w^2\rangle/\alpha\,, \tag{22}$$

where

$$\langle w^2\rangle \equiv \frac{\Delta(w_1 + w_2)/2}{\log(w_2/w_1)} = \frac{w_1^2 + w_2^2}{2}\left[1 + O\left(\frac{\Delta}{w_1}\right)^2\right]. \tag{23}$$

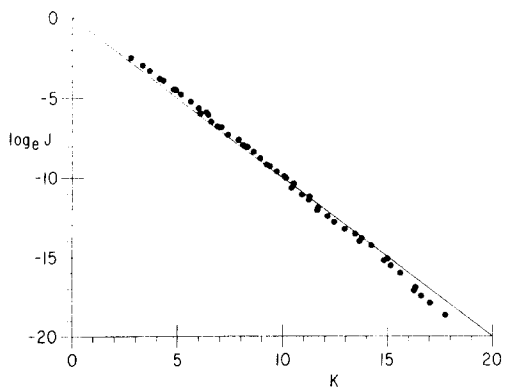

FIG. 9. A plot of $\log_e J$ against $K \equiv w_1^2/2 - \log_e[\Delta(w_1 + w_2)/(8\pi)^{1/2}]$. The dots give the numerical results. The line is the prediction of the one-dimensional theory, Eq. (18).

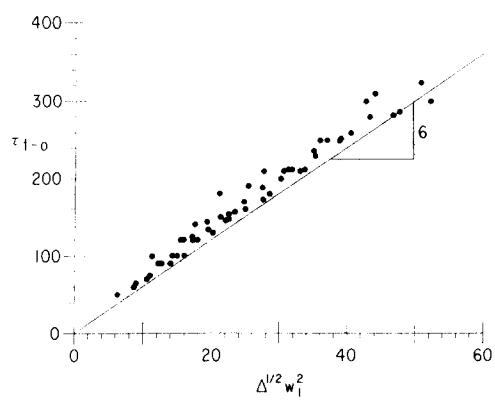

FIG. 10. The turn-on time, $\tau_{t\text{-}o}$, for the current as a function of of $\Delta^{1/2} w_1^2$.

Note that in Ref. 1, the collision frequency was incorrectly given.[6] Thus, the analysis of Ref. 1 uses $\alpha = 1$, although for $Z_i = 1$, α should be $\frac{3}{2}$. Figure 11 shows the dependence of J/P_d on $\langle w^2 \rangle$ numerically computed from the two-dimensional code. This gives

$$J/P_d \approx 1.7\langle w^2 \rangle , \tag{24}$$

which is 1.7 larger than the value predicted by Ref. 1 [Eq. (22) with $\alpha = 1$] or 2.5 larger than the correct one-dimensional result [Eq. (22) with $\alpha = \frac{3}{2}$]. While the discrepancy with the result of Ref. 1 is not great, this is the most important result of the present study. We will return to the implications of this result in the next section.

Finally, we briefly look at the dependence of J/P_d on D and Z_i. From the one-dimensional theory for $Dw_1^2 \gg \Delta$, J, and P_d should be independent of D. If we double the value of D in the example considered in Sec. V (i.e., let $D = 1$), then J increases by 5%, P_d by 3%, and J/P_d by 2%, confirming the one-dimensional analysis.

The dependence of the problem on Z_i is much more pronounced. The one-dimensional analysis implies that the effect of changing Z_i (from $Z_i = 1$) is to decrease J/P_d by a factor of $(2 + Z_i)/3$, as seen from Eq. (22). To numerically examine the dependence of J/P_d on Z_i, we ran the case $D = \frac{1}{2}$, $w_1 = 3$, $w_2 = 5$ with $Z_i = 3$ and $Z_i = 5$, comparing the results with the case $Z_i = 1$, discussed in Sec. V. The one-dimensional prediction is that for $Z_i = 1$, 3, and 5, J/P_d scales as $1 : \frac{3}{5} : \frac{3}{7}$. The two-dimensional numerical results reveal that this scaling should be $1 : 0.82 : 0.71$, i.e., J/P_d decreases more slowly with increasing Z_i than the one-dimensional theory predicts. As Z_i increases, the one-dimensional theory becomes less and less accurate, reflecting the increased importance of the two-dimensional velocity-space structure.[5] The greater than predicted J/P_d is a result of the large perpendicular flattening in the resonant region. The non-Maxwellian electrons, which are the ones that lose power to the bulk distribution through energy collisions, are at higher absolute velocities than the one-dimensional analytic theory assumed. Thus, they collide less frequently, dissipating less power, though carrying the same amount of current. At high Z_i, the flattening in perpendicular velocity space is greater, so that this effect, as expected, is all the more pronounced.

VII. CONCLUSIONS

We have numerically verified the most important predictions of the one-dimensional Fokker–Planck analysis. The most important verification is the confirmation that a new resistivity law holds for rf-excited currents wherein the power dissipated is proportional to the current rather than the square of the current. The proportionality constant scales as predicted, i.e., $1/\langle w^2 \rangle$, but our numerical analysis shows that the power dissipated is only 60% of the prediction of Ref. 1. This discrepancy, although slight, has important implications. In the building of steady-state tokamak reactors, the power requirements on the use of rf-driven currents

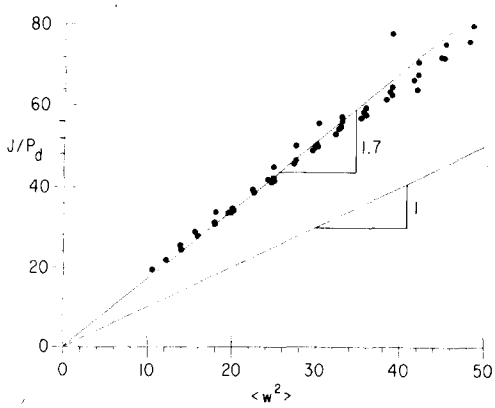

FIG. 11. A plot of J/P_d against $\langle w^2 \rangle$ [see Eq. (23)] for $Z_i = 1$. The dots give the numerical results. The line with a slope of unity is the one-dimensional prediction of Ref. 1.

was thought to be about 5% of the fusion power output. For very large and hence undesirable machines, this requirement could be reduced to about 3%. In any case, these power requirements, hinging on the efficiency of other components, are thought to be only marginally feasible. Our numerical work now shows that a more accurate prediction of the cost of the rf power is 40% lower than previously thought and could well brighten the prospect of economic feasibility.

The one-dimensional velocity-space model also predicted that the current in the steady state would be carried by a "raised plateau" of electrons and that this state would be reached on a collisional time scale. This picture is numerically shown to be correct, although the turn-on time for the current is substantially longer than predicted. We should emphasize, however, that although it is interesting to uncover and explain these discrepancies with the one-dimensional theory, the differences (other than in J/P_d) are not relevant to the problem of steady-state reactors. Any small enhancement of the current discovered numerically would be overshadowed, in practice, by even a very small displacement of the wave spectrum location in velocity space. Similarly, the increased length of the turn-on time is immaterial, of course, to the steady-state operation.

Finally, we would like to emphasize that our primary goal in this paper has been to numerically check the validity of the one-dimensional approximation, which appeared to be the most difficult to justify. Our numerical work still retains a number of other approximations regarding, for example, the nature of the background distributions. Thus, even in the steady-state spatially homogeneous problem, considering only Coulomb collisions and resonant diffusion effects, there remains room for an improved posing of the problem and further numerical work, although no drastic changes in the present results are expected.

ACKNOWLEDGMENTS

The computer program used for the solution of the Fokker–Planck equation was developed by R. M. Kuls-

rud, Y. -C. Sun, N. Winsor, and H. A. Fallon, and is based on a program by J. Killeen and K. D. Marx.[7] The authors wish to thank Y.-C. Sun for helping them get the program running. The work of one of the authors (NJF) was begun while he was at the Research Laboratory of Electronics at the Massachusetts Institute of Technology and he wishes to thank Professor W. B. Davenport, Jr. and Professor P. A. Wolff for their support and encouragement of this work.

This work was supported by the United States Department of Energy Contract Nos. EY-76-C-02-3073 and EG-77-G-01-4107.

[1]N. J. Fisch, Phys. Rev. Lett. **41**, 873 (1978).
[2]C. F. Kennel and F. Engelmann, Phys. Fluids **9**, 2377 (1966).
[3]B. A. Trubnikov, in *Reviews of Plasma Physics*, edited by M. A. Leontovich (Consultants Bureau, New York, 1965), Vol. 1, p. 105.
[4]A. A. Vedenov, in *Reviews of Plasma Physics*, edited by M. A. Leontovich (Consultants Bureau, New York, 1967), Vol. 3, p. 229.
[5]N. J. Fisch, Ph.D. thesis, Massachusetts Institute of Technology (1978).
[6]N. J. Fisch, Phys. Rev. Lett. **42**, 410 (1979).
[7]J. Killeen and K. D. Marx, in *Methods of Computational Physics*, edited by B. Adler, S. Fernbach, and M. Rotenberg (Academic, New York, 1970), Vol. 9, p. 422.